Pathological basis for deficient excitatory drive to cortical parvalbumin interneurons in schizophrenia

Daniel W. Chung, MS[a,b], **Kenneth N. Fish, PhD**[a], and **David A. Lewis, MD**[a]

[a]Translational Neuroscience Program, Department of Psychiatry, University of Pittsburgh, Pittsburgh, PA

[b]Medical Scientist Training Program, University of Pittsburgh School of Medicine, Pittsburgh, PA

Abstract

Objective—Deficient excitatory drive to parvalbumin-containing cortical interneurons is proposed to serve as a key neural substrate for altered gamma oscillations and cognitive dysfunction in schizophrenia. However, a pathological entity producing such a deficit has not yet been identified. In this study, we tested the hypothesis that cortical parvalbumin interneurons receive fewer excitatory synaptic inputs in individuals with schizophrenia.

Method—Fluorescent immunohistochemistry, confocal microscopy and post-image processing techniques were used to quantify the number of vesicular glutamate transporter 1-positive (VGlut1+)/postsynaptic density protein 95-positive (PSD95+) puncta (putative excitatory synapses) per surface area of parvalbumin-positive (PV+) or calretinin-positive (CR+) neurons in the dorsolateral prefrontal cortex from schizophrenia subjects and matched unaffected comparison subjects.

Results—Mean density of VGlut1+/PSD95+ puncta on PV+ neurons was significantly 18% lower in schizophrenia subjects. This deficit was not influenced by methodological confounds or schizophrenia-associated comorbid factors, not present in monkeys chronically exposed to psychotropic medications, and not present in CR+ neurons. The mean density of VGlut1+/PSD95+ puncta on PV+ neurons predicted the activity-dependent expression levels of parvalbumin and glutamic acid decarboxylase 67 (GAD67) in schizophrenia subjects but not in comparison subjects.

Conclusions: Here we demonstrate for the first time that the density of excitatory synapses is lower selectively on parvalbumin interneurons in schizophrenia and predicts the activity-dependent down-regulation of parvalbumin and GAD67 levels. Because the activity of parvalbumin interneurons is required for the generation of cortical gamma oscillations and working memory function, these findings reveal a novel pathological substrate for cortical dysfunction and cognitive deficits in schizophrenia.

Corresponding author: David A. Lewis, M.D., Department of Psychiatry, University of Pittsburgh, BST W1653, 3811 O'Hara St., Pittsburgh, PA 15213, Tel: 412-246-6010; Fax: 412-624-9910, lewisda@upmc.edu.

disclosures

All other authors report no biomedical financial interests or potential conflicts of interest.

Introduction

Cognitive dysfunction is a core and clinically-critical feature of schizophrenia[1] but responds poorly to available medications[2]. Therefore, identifying the neural substrate for these cognitive deficits is critical for the development of new therapeutic interventions. Certain cognitive deficits, such as impaired working memory, appear to emerge from altered gamma oscillations in the dorsolateral prefrontal cortex (DLPFC)[3]. Because cortical gamma oscillations require the activity of parvalbumin-containing (PV) interneurons[4, 5], deficient cortical PV interneuron activity could provide the neural substrate for altered prefrontal gamma oscillations and consequently impaired working memory in schizophrenia.

Lower glutamatergic drive to PV interneurons has been hypothesized to be the cause of deficient PV interneuron activity in schizophrenia[6-8]. This hypothesis is based on findings that experimental manipulations in model systems which reduce glutamatergic drive to PV interneurons result in lower PV interneuron activity accompanied by lower expression of activity-dependent gene products (e.g., PV and the GABA-synthesizing enzyme glutamic acid decarboxylase 67, GAD67), abnormal gamma oscillations and working memory deficits[9-12]. Consistent with this hypothesis, postmortem studies have repeatedly shown lower PV and GAD67 levels in the DLPFC of schizophrenia subjects[13-17], which are thought to reflect lower glutamatergic drive to a subset of PV neurons and not a loss of PV neurons in the illness[13, 15, 18, 19]. These deficits do not seem to be due to a global reduction in excitatory drive to all interneuron subtypes, as calretinin-containing (CR) interneurons, the most abundant interneuron subtype in the primate DLPFC[20], appear to be relatively unaffected in schizophrenia[15, 16, 21]. However, the pathological basis for lower glutamatergic drive selectively onto PV interneurons, such as fewer excitatory synapses on these neurons, has not been identified in people with schizophrenia.

Therefore, in this study, we used multi-labeling fluorescent immunohistochemistry, confocal imaging and a custom post-image processing method to directly assess excitatory synapses on parvalbumin-positive (PV+) neurons in the DLPFC from matched pairs of schizophrenia and unaffected comparison subjects. We tested the hypotheses that 1) lower PV levels in subjects with schizophrenia reflect altered PV expression per neuron and not a loss of PV+ neurons; 2) PV+, but not calretinin-positive (CR+), neurons receive fewer excitatory synaptic inputs in subjects with schizophrenia; and 3) fewer excitatory synapses on PV+ neurons are associated with activity-dependent down-regulation of PV and GAD67 levels.

Materials and Methods

Human Subjects

Brain specimens (N=40) were obtained during routine autopsies conducted at the Allegheny County Office of the Medical Examiner (Pittsburgh, PA) after consent was obtained from the next-of-kin. An independent team of clinicians made consensus DSM-IV diagnoses for each subject based on structured interviews with family members and review of medical records. The absence of a psychiatric diagnosis was confirmed in unaffected comparison subjects using the same approach. All procedures were approved by the University of Pittsburgh

Committee for the Oversight of Research and Clinical Training Involving the Dead and the Institutional Review Board for Biomedical Research. The subjects were selected based on a postmortem interval (PMI) less than 24 hours in order to avoid the effect of PMI on protein immunoreactivity (**Supplementary Methods**). In addition, to control for the autofluorescence emitted by lipofuscin which accumulates with aging[22], all subjects were less than 62 years of age. To control for experimental variance and to reduce biological variance, each subject with schizophrenia or schizoaffective disorder (N=20) was paired with one unaffected comparison subject for sex and as closely as possible for age (**Supplementary Table S1**). The mean age, PMI and tissue storage time did not differ between subject groups (**Table 1**).

Fluorescent Immunohistochemistry

Paraformaldehyde-fixed coronal tissue sections (40μm) containing DLPFC area 9 were processed for fluorescent immunohistochemistry as previously described[23]. Sections were pretreated for antigen retrieval (0.01M sodium citrate for 75 minutes at 80°C) and then incubated for 72 hours in the following primary antibodies: PV (mouse, 1:1000, Swant, Bellinzona, Switzerland), CR (goat, 1:1000, Swant), post-synaptic density 95 (PSD95; rabbit, 1:250, Cell Signaling, Danvers, MA) and vesicular glutamate transporter 1 (VGlut1; guinea pig, 1:250, Millipore, Billerica, MA). Tissue sections were then incubated for 24 hours with secondary antibodies (donkey) conjugated to Alexa 488 (anti-mouse, 1:500), 568 (anti-rabbit, 1:500), 647 (anti-guinea pig, 1:500, all from Invitrogen, Carlsbad, CA) or biotin (anti-goat, 1:200, Fitzgerald, Acton, MA). Sections were then incubated with streptavidin 405 (1:200, invitrogen) for 24 hours. After washing, sections were mounted in the Prolong Gold Antifade reagent (Life technologies, Carlsbad, CA), coded to obscure diagnosis and subject number, and stored at 4°C until imaging. All antibodies used in this study have been previously shown to specifically recognize the targeted protein (**Supplementary Methods**).

Image Acquisition

Images were acquired on an Olympus (Center Valley, PA, USA) IX81 inverted microscope equipped with an Olympus spinning disk confocal unit, a Hamamatsu EM-CCD digital camera (Bridgewater, NJ, USA), and a high-precision BioPrecision2 XYZ motorized stage with linear XYZ encoders (Ludl Electronic Products Ltd, Hawthorne, NJ, USA) using a 60x 1.40 NA SC oil immersion objective. Ten image stacks (512×512 pixels; 0.25 μm z-step) in layer 2 or 4 from each section were selected using a previously published method for systematic random sampling[24]. Layer 2 or 4 was defined as 10-20% or 50-60% of the pia-to-white matter distance, respectively[25]. We sampled these two layers as layer 4 contains a high density of PV interneurons[20] and prominently lower PV mRNA levels in schizophrenia[15, 21], whereas layer 2 contains a high density of CR interneurons[26]. The very low densities of PV interneurons in layer 2 and of CR interneurons in layer 4 precluded the sampling of these neurons. Lipofuscin for each stack was imaged using a custom fifth channel (excitation wavelength: 405nm; emission wavelength: 647nm) at a constant exposure time as previously described[27].

Post-image Processing and Object Sampling

Each fluorescent channel was deconvolved using the Autoquant's Blind Deconvolution algorithm to improve resolving power. VGlut1+ and PSD95+ puncta were used to identify the pre- and postsynaptic elements, respectively, as these molecular markers have been previously used to define excitatory synapses in PV interneurons(11, 28, 29). Masking of VGlut1+ and PSD95+ puncta was performed using the previously described method (**Supplementary Methods and Supplementary Figure S1**). Edges of PV+ or CR+ cell bodies were segmented by the MATLAB edge function using the Canny edge detector operator(30). The edges of segmented objects were closed, filled and size-gated ($>80\mu m^3$) to limit the boundaries of PV+ or CR+ cell bodies. All PV+ and CR+ cell body masks were manually cleaned for final analyses (**Supplementary Figure S1**). We sampled objects that localized within the middle 80% of z-planes (~32 μm), based on antibody penetration efficiency analyses to avoid edge effects (**Supplementary Methods**). The mean volume of tissue sampled did not differ between subject groups (layer 2: $t_{19}=0.3$, p=0.776; layer 4: $t_{19}=0.03$, p=0.998). The mean numbers of VGlut1+ puncta and PSD95+ puncta sampled in layer 2 or layer 4 did not differ between subject groups (all $t_{19}<|1.6|$, all p>0.12), indicating the absence of any group differences in cortical lamination. Numbers of VGlut1+/PSD95+ puncta per surface area of PV+ or CR+ cell bodies were calculated in order to determine the density of excitatory synapses on PV+ or CR+ neurons.

Antipsychotic-Exposed Monkeys

Male monkeys (*Macaca fasicularis*) received oral doses of haloperidol (12–14 mg), olanzapine (5.5–6.6 mg) or placebo (N=6 per each group) twice daily for 17-27 months as previously described(31). Trough plasma levels for haloperidol and olanzapine were within the range associated with clinical efficacy in humans(31). Monkeys were euthanized in triads (one monkey from each of the three groups) on the same day. Coronal sections (40 μm) containing DLPFC area 9 from each monkey were processed for fluorescent immunohistochemistry as described above.

Statistics

Two analyses of covariance (ANCOVA) models were used to assess the main effect of diagnosis on the dependent measures. The paired ANCOVA model included subject pair as a blocking factor, and PMI and tissue storage time as covariates. This paired model accounts both for our attempts to balance diagnostic groups for sex and age and for the parallel tissue processing of both subjects in a pair, but is not a true statistical paired design. Therefore, we also used an unpaired ANCOVA model that included sex, age, PMI and storage time as covariates. Most covariates were not significant and therefore were not included in the final analyses; exceptions included an effect of tissue storage time on the mean density of PSD95+ puncta on PV+ cell bodies ($F_{1,35}=5.5$;p=0.025) by unpaired ANCOVA and an effect of storage time on the mean surface area of CR+ cell bodies ($F_{1,18}=6.5$;p=0.021) and on the mean density of VGlut1+/PSD95+ puncta on CR+ cell bodies ($F_{1,18}=8.8$;p=0.008) by paired ANCOVA.

The potential influence of co-morbid factors (e.g., diagnosis of schizoaffective disorder; history of substance dependence or abuse; nicotine use, antidepressant, or benzodiazepine

and/or sodium valproate use at time of death; death by suicide) in the schizophrenia subjects was assessed by an ANCOVA model with each factor as the main effect and sex, age, PMI and storage time as covariates. Pearson's correlation analysis was performed to assess the relationships between the density of VGlut1+/PSD95+ puncta on PV+ cell bodies and somal PV immunoreactivity levels or PV and GAD67 mRNA levels obtained from previously published studies(32, 33). For the antipsychotic-exposed monkeys, an ANCOVA was used to assess the main effect of antipsychotic treatment on the dependent measures with triad as a blocking factor.

Results

PV levels are lower in a subset of PV interneurons in schizophrenia

We sampled PV+ neurons in DLPFC layer 4 (**Figure 1A,B**), as lower PV mRNA levels in schizophrenia are prominent in this layer(15, 21). Consistent with those findings, mean PV protein levels in PV+ cell bodies were significantly 34% lower in subjects with schizophrenia (**Figure 1C**). The mean numbers of PV+ neurons in identical volumes of sampled tissue did not differ between subject groups (**Figure 1D**). Finally, we observed a left shift in the frequency distribution of PV levels per PV+ cell body in schizophrenia subjects relative to comparison subjects (**Figure 1E**). Together, these findings suggest that lower PV levels in schizophrenia reflect lower PV expression in a subset of PV neurons and not a deficit in PV neuron number.

PV interneurons receive fewer excitatory synaptic inputs in schizophrenia

The pre- and postsynaptic elements of excitatory synapses on PV+ neurons were identified by VGlut1+ puncta and PSD95+ puncta, respectively (**Figure 2A,B**). Excitatory synapses were defined by the overlap of VGlut1+ and PSD95+ (VGlut1+/PSD95+) puncta. The mean density of VGlut1+/PSD95+ puncta on PV+ cell bodies was significantly 18% lower in schizophrenia subjects (**Figure 2C**). The mean densities of VGlut1+ or PSD95+ puncta on PV+ cell bodies were also significantly 12% or 19% lower, respectively, in schizophrenia subjects (**Figure 2D,E**), reflecting fewer pre- and postsynaptic glutamatergic structures on PV+ neurons.

Fewer excitatory synapses on PV interneurons are not affected by methodological confounds or disease-associated co-morbid factors

The mean surface area of PV+ cell bodies did not differ between subject groups (**Figure 2F**), indicating that the lower density of excitatory synapses on PV+ neurons in schizophrenia is not due to a larger surface area of PV+ cell bodies. The mean VGlut1 or PSD95 protein levels in labeled puncta on PV+ cell bodies did not differ between subject groups (**Supplementary Figure S2C,D**), suggesting that our findings of fewer synaptic structures in schizophrenia were not biased by lower levels of synaptic markers. Finally, the mean density of VGlut1+/PSD95+ puncta on PV+ cell bodies did not differ among schizophrenia subjects as a function of assessed co-morbid factors (**Supplementary Figure S3**) and was not altered in monkeys chronically exposed to psychotropic medications (**Supplementary Figure S4D**). Together, these findings suggest that fewer excitatory

synapses on PV+ neurons reflect the disease process of schizophrenia, and are not due to methodological confounds or other factors commonly associated with the illness.

CR interneurons do not receive fewer excitatory synaptic inputs in schizophrenia

In order to determine the cell type-specificity of fewer excitatory synapses on PV+ neurons, we measured the density of excitatory synapses on CR+ neurons. The mean numbers of sampled CR+ neurons, mean somal CR protein levels and mean surface area of CR+ cell bodies did not differ between subject groups (**Figure 3A-C**). The mean density of VGlut1+/PSD95+ puncta on CR+ cell bodies was non-significantly 9% higher in schizophrenia subjects (**Figure 3D**), demonstrating that the number of excitatory synapses on CR+ neurons is not lower in the illness.

Validation of methods for quantifying excitatory synaptic inputs

We have previously shown by duel-labeling electron microscopy that the density of excitatory synapses is significantly 1.90 fold higher on PV+ than CR+ neurons in the primate DLPFC(34). Consistent with these findings, the mean density of VGlut1+/PSD95+ puncta on PV+ cell bodies was significantly (t_{19}=8.5, p<0.001) 1.73 fold higher than on CR+ cell bodies in the comparison subjects in the present study. This finding indicates that the light microscopic methods used here provide a robust means for sampling excitatory synaptic inputs specific to PV+ or CR+ neurons.

Excitatory synapses on PV interneurons predict PV and GAD67 expression levels in human DLPFC

Finally, we assessed whether the density of excitatory synapses on PV+ neurons predicted levels of PV and GAD67, molecular markers of PV interneuron activity. Mean density of VGlut1+/PSD95+ puncta on PV+ cell bodies was positively correlated with PV and GAD67 mRNA levels in schizophrenia subjects but not in comparison subjects (**Figure 4A,B**). In addition, the mean density of VGlut1+/PSD95+ puncta on PV+ cell bodies positively predicted the mean somal PV immunoreactivity levels in schizophrenia subjects but not in comparison subjects (**Figure 4C**). Moreover, this positive correlation was evident across all sampled PV+ neurons in both subject groups (**Figure 4D**). Among these neurons, the PV+ neurons with the lowest PV levels (more than one standard deviation below the mean) had a density of VGlut1+/PSD95+ puncta significantly (t_{112}=-5.4; p<0.001) 42% lower than the PV+ neurons with the highest PV levels (more than one standard deviation above the mean).

Discussion

A pathological substrate for reduced glutamatergic drive onto PV interneurons in schizophrenia has not been previously identified due to the technical challenges of resolving synaptic abnormalities in a cell type-specific manner in postmortem human brain. Here, we report for the first time that the neuropathology of schizophrenia includes a lower number of excitatory synapses on PV interneurons. This deficit appears to reflect the disease process of schizophrenia and is not due to methodological confounds or other factors commonly associated with the illness. First, fewer excitatory synapses on PV+ neurons was evident from lower numbers of both pre- and postsynaptic markers, validating deficits in the

synaptic structures. Second, these deficits were not confounded by either a larger surface area of PV+ cell bodies or undetectable levels of protein markers within existing synaptic structures in schizophrenia subjects. Third, none of the assessed schizophrenia-associated co-morbid factors accounted for these deficits. Fourth, long-term exposure to psychotropic medications did not alter the density of excitatory synapses on PV+ neurons in the DLPFC of non-human primates; the effect of antipsychotics could not be assessed in humans as only one schizophrenia subject had not been exposed to these medications. Fifth, the density of excitatory synapses on CR+ neurons was not lower in the illness, consistent with a prominent pathology of PV interneurons in schizophrenia. Finally, the density of excitatory synapses on PV+ neurons predicted levels of the activity-dependent gene products PV and GAD67 selectively in the schizophrenia subjects. Together, these findings support the hypothesis that fewer excitatory synapses selectively on cortical PV interneurons provide a pathological substrate for deficient excitatory drive to these interneurons in schizophrenia.

PV interneurons comprise two main subtypes: PV basket neurons target the proximal dendrites and cell bodies of pyramidal neurons and PV chandelier neurons synapse onto the axon initial segment of pyramidal neurons(35). Although both populations of PV interneuron subtypes are active during gamma oscillations, gamma rhythms are more strongly coupled to the activity of PV basket neurons(36, 37). Given the much greater prevalence of PV basket neurons in the middle layers of the primate DLPFC(38, 39), most of the PV+ neurons sampled in our study are likely to be PV basket neurons.

Our sampling of excitatory synapses on PV+ neurons is limited in two respects. First, we did not sample vesicular glutamate transporter 2-containing excitatory inputs that represent projections from the thalamus(40). However, thalamic axons represent a small minority (<10%) of excitatory terminals in the cortex(41) and only a small percentage of thalamic inputs target PV interneurons(42), suggesting that the excitation of PV interneurons is mostly driven by cortical excitatory inputs. Second, we did not sample synaptic inputs to dendrites of PV interneurons due to the few dendrites originating from PV+ cell bodies, with detectable PV immunoreactivity. Although the density of excitatory synapses is higher onto dendrites than cell bodies of PV interneurons(30), depolarization of the cell body of PV interneurons is much stronger for somal than dendritic excitatory inputs(31,32). However, despite these limitations, the density of excitatory cortical synapses on PV+ cell bodies in the present study predicted activity-dependent PV expression across all PV+ neurons. Therefore, our approach was sufficiently sensitive to detect an apparently functionally meaningful deficit in excitatory synaptic inputs to PV+ neurons in schizophrenia subjects.

Multiple signaling pathways regulate the formation of excitatory synapses on PV interneurons. For example, the ErbB4 signaling pathway induces the formation of excitatory synapses on PV interneurons(11, 43, 44) and the release of neuronal pentraxin 2 (Narp) from pyramidal cells recruits excitatory synapses selectively on PV interneurons in an activity-dependent manner(28). Both an abnormal shift in ErbB4 splicing at the JM locus(45, 46) and lower Narp transcript levels have been shown in the DLPFC of subjects with schizophrenia, including those included in the present study(21, 47). Across these subjects, the density of VGlut1+/PSD95+ puncta on PV+ cell bodies was significantly correlated with the ratio of ErbB4 JM-a to JM-b splice variants in cortical layer 4 (R=-0.436, p=0.005) and

with Narp mRNA levels in total gray matter (R=0.351, p=0.026). These findings suggest that alterations in the ErbB4 and/or Narp signaling pathways could be upstream of the deficit in excitatory synaptic inputs to, and consequently the lower activity of, PV interneurons in schizophrenia.

Consistent with the idea that PV interneuron activity is reduced in the illness, activity-dependent expression levels of GAD67 are lower in the DLPFC of subjects with schizophrenia, and specifically in PV interneurons(14, 17). Experimental reductions of GAD67 in PV interneurons decrease inhibitory synaptic transmission in pyramidal cells and alter cortical network activity(48-50). Strong inhibition of pyramidal cells by PV interneurons is required for the generation of gamma oscillations in the DLPFC associated with working memory. Thus, the lower density of excitatory synapses on PV+ neurons and the corresponding deficit in GAD67 expression found in the present study could provide a pathological substrate for deficient inhibition of pyramidal cells by PV interneurons, which in turn would result in impaired gamma oscillations and working memory deficits in people with schizophrenia.

Discovering pathological entities that bridge etiopathogenic pathways to the core features of the illness is essential for understanding the disease process of schizophrenia. For example, disruptions in the ErbB4 or Narp signaling pathways in the DLFPC could be upstream of the deficits in excitatory synaptic inputs to PV interneurons in schizophrenia. Given that PV interneuron activity is essential for gamma oscillations, these deficits could underlie the downstream pathophysiology of impaired gamma oscillations and consequently working memory dysfunction in schizophrenia. Therefore, fewer excitatory synapses on PV interneurons might serve as a common pathological locus upon which diverse streams of etiopathogenic pathways converge in order to produce a core pathophysiological feature of schizophrenia from which cognitive dysfunction emerges.

Supplementary Material

Refer to Web version on PubMed Central for supplementary material.

Acknowledgement

References

1. Kahn RS, Keefe RS. Schizophrenia is a cognitive illness: time for a change in focus. JAMA Psychiatry. 2013; 70:1107–1112. [PubMed: 23925787]

2. Keefe RS, Harvey PD. Cognitive impairment in schizophrenia. Handb Exp Pharmacol. 2012:11–37. [PubMed: 23027411]

3. Uhlhaas PJ, Singer W. Abnormal neural oscillations and synchrony in schizophrenia. Nat Rev Neurosci. 2010; 11:100–113. [PubMed: 20087360]

4. Sohal VS, Zhang F, Yizhar O, Deisseroth K. Parvalbumin neurons and gamma rhythms enhance cortical circuit performance. Nature. 2009; 459:698–702. [PubMed: 19396159]

5. Cardin JA, Carlen M, Meletis K, Knoblich U, Zhang F, Deisseroth K, Tsai LH, Moore CI. Driving fast-spiking cells induces gamma rhythm and controls sensory responses. Nature. 2009; 459:663–667. [PubMed: 19396156]

6. Coyle JT, Basu A, Benneyworth M, Balu D, Konopaske G. Glutamatergic synaptic dysregulation in schizophrenia: therapeutic implications. Handb Exp Pharmacol. 2012:267–295.

7. Moghaddam B, Krystal JH. Capturing the angel in "angel dust": twenty years of translational neuroscience studies of NMDA receptor antagonists in animals and humans. Schizophr Bull. 2012; 38:942–949. [PubMed: 22899397]

8. Gonzalez-Burgos G, Lewis DA. NMDA receptor hypofunction, parvalbumin-positive neurons, and cortical gamma oscillations in schizophrenia. Schizophr Bull. 2012; 38:950–957. [PubMed: 22355184]

9. Behrens MM, Ali SS, Dao DN, Lucero J, Shekhtman G, Quick KL, Dugan LL. Ketamine-induced loss of phenotype of fast-spiking interneurons is mediated by NADPH-oxidase. Science. 2007; 318:1645–1647. [PubMed: 18063801]

10. Belforte JE, Zsiros V, Sklar ER, Jiang Z, Yu G, Li Y, Quinlan EM, Nakazawa K. Postnatal NMDA receptor ablation in corticolimbic interneurons confers schizophrenia-like phenotypes. Nat Neurosci. 2010; 13:76–83. [PubMed: 19915563]

11. Del Pino I, Garcia-Frigola C, Dehorter N, Brotons-Mas JR, Alvarez-Salvado E, Martinez de Lagran M, Ciceri G, Gabaldon MV, Moratal D, Dierssen M, Canals S, Marin O, Rico B. Erbb4 Deletion from Fast-Spiking Interneurons Causes Schizophrenia-like Phenotypes. Neuron. 2013; 79:1152–1168. [PubMed: 24050403]

12. Pelkey KA, Barksdale E, Craig MT, Yuan X, Sukumaran M, Vargish GA, Mitchell RM, Wyeth MS, Petralia RS, Chittajallu R, Karlsson RM, Cameron HA, Murata Y, Colonnese MT, Worley PF, McBain CJ. Pentraxins coordinate excitatory synapse maturation and circuit integration of parvalbumin interneurons. Neuron. 2015; 85:1257–1272. [PubMed: 25754824]

13. Akbarian S, Kim JJ, Potkin SG, Hagman JO, Tafazzoli A, Bunney WE Jr. Jones EG. Gene expression for glutamic acid decarboxylase is reduced without loss of neurons in prefrontal cortex of schizophrenics. Arch Gen Psychiatry. 1995; 52:258–266. [PubMed: 7702443]

14. Volk DW, Austin MC, Pierri JN, Sampson AR, Lewis DA. Decreased glutamic acid decarboxylase67 messenger RNA expression in a subset of prefrontal cortical gamma-aminobutyric acid neurons in subjects with schizophrenia. Arch Gen Psychiatry. 2000; 57:237–245. [PubMed: 10711910]

15. Hashimoto T, Volk DW, Eggan SM, Mirnics K, Pierri JN, Sun Z, Sampson AR, Lewis DA. Gene expression deficits in a subclass of GABA neurons in the prefrontal cortex of subjects with schizophrenia. J Neurosci. 2003; 23:6315–6326. [PubMed: 12867516]

16. Fung SJ, Webster MJ, Sivagnanasundaram S, Duncan C, Elashoff M, Weickert CS. Expression of interneuron markers in the dorsolateral prefrontal cortex of the developing human and in schizophrenia. Am J Psychiatry. 2010; 167:1479–1488. [PubMed: 21041246]

17. Curley AA, Arion D, Volk DW, Asafu-Adjei JK, Sampson AR, Fish KN, Lewis DA. Cortical deficits of glutamic acid decarboxylase 67 expression in schizophrenia: clinical, protein, and cell type-specific features. Am J Psychiatry. 2011; 168:921–929. [PubMed: 21632647]

18. Woo TU, Miller JL, Lewis DA. Schizophrenia and the parvalbumin-containing class of cortical local circuit neurons. Am J Psychiatry. 1997; 154:1013–1015. [PubMed: 9210755]

19. Enwright JF, Sanapala S, Foglio A, Berry R, Fish KN, Lewis DA. Reduced Labeling of Parvalbumin Neurons and Perineuronal Nets in the Dorsolateral Prefrontal Cortex of Subjects with Schizophrenia. Neuropsychopharmacology. 2016

20. Conde F, Lund JS, Jacobowitz DM, Baimbridge KG, Lewis DA. Local circuit neurons immunoreactive for calretinin, calbindin D-28k or parvalbumin in monkey prefrontal cortex: distribution and morphology. J Comp Neurol. 1994; 341:95–116. [PubMed: 8006226]

21. Chung DW, Volk DW, Arion D, Zhang Y, Sampson AR, Lewis DA. Dysregulated ErbB4 Splicing in Schizophrenia: Selective Effects on Parvalbumin Expression. Am J Psychiatry. 2016; 173:60–68. [PubMed: 26337038]

22. Porta EA. Pigments in aging: an overview. Ann N Y Acad Sci. 2002; 959:57–65. [PubMed: 11976186]

23. Glausier JR, Fish KN, Lewis DA. Altered parvalbumin basket cell inputs in the dorsolateral prefrontal cortex of schizophrenia subjects. Mol Psychiatry. 2014; 19:30–36. [PubMed: 24217255]

24. Sweet RA, Henteleff RA, Zhang W, Sampson AR, Lewis DA. Reduced dendritic spine density in auditory cortex of subjects with schizophrenia. Neuropsychopharmacology. 2009; 34:374–389. [PubMed: 18463626]

25. Pierri JN, Chaudry AS, Woo TU, Lewis DA. Alterations in chandelier neuron axon terminals in the prefrontal cortex of schizophrenic subjects. Am J Psychiatry. 1999; 156:1709–1719. [PubMed: 10553733]

26. Gabbott PL, Jays PR, Bacon SJ. Calretinin neurons in human medial prefrontal cortex (areas 24a,b,c, 32', and 25). J Comp Neurol. 1997; 381:389–410. [PubMed: 9136798]

27. Rocco BR, Lewis DA, Fish KN. Markedly Lower Glutamic Acid Decarboxylase 67 Protein Levels in a Subset of Boutons in Schizophrenia. Biol Psychiatry. 2015

28. Chang MC, Park JM, Pelkey KA, Grabenstatter HL, Xu D, Linden DJ, Sutula TP, McBain CJ, Worley PF. Narp regulates homeostatic scaling of excitatory synapses on parvalbumin-expressing interneurons. Nat Neurosci. 2010; 13:1090–1097. [PubMed: 20729843]

29. Donato F, Rompani SB, Caroni P. Parvalbumin-expressing basket-cell network plasticity induced by experience regulates adult learning. Nature. 2013; 504:272–276. [PubMed: 24336286]

30. Canny J. A Computational Approach to Edge-Detection. Ieee T Pattern Anal. 1986; 8:679–698.

31. Dorph-Petersen KA, Pierri JN, Perel JM, Sun Z, Sampson AR, Lewis DA. The influence of chronic exposure to antipsychotic medications on brain size before and after tissue fixation: a comparison of haloperidol and olanzapine in macaque monkeys. Neuropsychopharmacology. 2005; 30:1649–1661. [PubMed: 15756305]

32. Kimoto S, Bazmi HH, Lewis DA. Lower expression of glutamic acid decarboxylase 67 in the prefrontal cortex in schizophrenia: contribution of altered regulation by Zif268. Am J Psychiatry. 2014; 171:969–978. [PubMed: 24874453]

33. Volk DW, Chitrapu A, Edelson JR, Lewis DA. Chemokine receptors and cortical interneuron dysfunction in schizophrenia. Schizophr Res. 2015; 167:12–17. [PubMed: 25464914]

34. Melchitzky DS, Lewis DA. Pyramidal neuron local axon terminals in monkey prefrontal cortex: differential targeting of subclasses of GABA neurons. Cereb Cortex. 2003; 13:452–460. [PubMed: 12679292]

35. Williams SM, Goldman-Rakic PS, Leranth C. The synaptology of parvalbumin-immunoreactive neurons in the primate prefrontal cortex. J Comp Neurol. 1992; 320:353–369. [PubMed: 1613130]

36. Massi L, Lagler M, Hartwich K, Borhegyi Z, Somogyi P, Klausberger T. Temporal dynamics of parvalbumin-expressing axo-axonic and basket cells in the rat medial prefrontal cortex in vivo. J Neurosci. 2012; 32:16496–16502. [PubMed: 23152631]

37. Dugladze T, Schmitz D, Whittington MA, Vida I, Gloveli T. Segregation of axonal and somatic activity during fast network oscillations. Science. 2012; 336:1458–1461. [PubMed: 22700932]

38. Krimer LS, Zaitsev AV, Czanner G, Kroner S, Gonzalez-Burgos G, Povysheva NV, Iyengar S, Barrionuevo G, Lewis DA. Cluster analysis-based physiological classification and morphological properties of inhibitory neurons in layers 2-3 of monkey dorsolateral prefrontal cortex. J Neurophysiol. 2005; 94:3009–3022. [PubMed: 15987765]

39. Zaitsev AV, Gonzalez-Burgos G, Povysheva NV, Kroner S, Lewis DA, Krimer LS. Localization of calcium-binding proteins in physiologically and morphologically characterized interneurons of monkey dorsolateral prefrontal cortex. Cereb Cortex. 2005; 15:1178–1186. [PubMed: 15590911]

40. Fremeau RT Jr. Troyer MD, Pahner I, Nygaard GO, Tran CH, Reimer RJ, Bellocchio EE, Fortin D, Storm-Mathisen J, Edwards RH. The expression of vesicular glutamate transporters defines two classes of excitatory synapse. Neuron. 2001; 31:247–260. [PubMed: 11502256]

41. Latawiec D, Martin KA, Meskenaite V. Termination of the geniculocortical projection in the striate cortex of macaque monkey: a quantitative immunoelectron microscopic study. J Comp Neurol. 2000; 419:306–319. [PubMed: 10723007]

42. Rotaru DC, Barrionuevo G, Sesack SR. Mediodorsal thalamic afferents to layer III of the rat prefrontal cortex: synaptic relationships to subclasses of interneurons. J Comp Neurol. 2005; 490:220–238. [PubMed: 16082676]

43. Ting AK, Chen Y, Wen L, Yin DM, Shen C, Tao Y, Liu X, Xiong WC, Mei L. Neuregulin 1 promotes excitatory synapse development and function in GABAergic interneurons. J Neurosci. 2011; 31:15–25. [PubMed: 21209185]

44. Mei L, Nave KA. Neuregulin-ERBB signaling in the nervous system and neuropsychiatric diseases. Neuron. 2014; 83:27–49. [PubMed: 24991953]

45. Law AJ, Kleinman JE, Weinberger DR, Weickert CS. Disease-associated intronic variants in the ErbB4 gene are related to altered ErbB4 splice-variant expression in the brain in schizophrenia. Hum Mol Genet. 2007; 16:129–141. [PubMed: 17164265]

46. Joshi D, Fullerton JM, Weickert CS. Elevated ErbB4 mRNA is related to interneuron deficit in prefrontal cortex in schizophrenia. J Psychiatr Res. 2014; 53:125–132. [PubMed: 24636039]

47. Kimoto S, Zaki MM, Bazmi HH, Lewis DA. Altered Markers of Cortical gamma-Aminobutyric Acid Neuronal Activity in Schizophrenia: Role of the NARP Gene. JAMA Psychiatry. 2015; 72:747–756. [PubMed: 26038830]

48. Lazarus MS, Krishnan K, Huang ZJ. GAD67 deficiency in parvalbumin interneurons produces deficits in inhibitory transmission and network disinhibition in mouse prefrontal cortex. Cereb Cortex. 2015; 25:1290–1296. [PubMed: 24275833]

49. Brown JA, Ramikie TS, Schmidt MJ, Baldi R, Garbett K, Everheart MG, Warren LE, Gellert L, Horvath S, Patel S, Mirnics K. Inhibition of parvalbumin-expressing interneurons results in complex behavioral changes. Mol Psychiatry. 2015; 20:1499–1507. [PubMed: 25623945]

50. Georgiev D, Yoshihara T, Kawabata R, Matsubara T, Tsubomoto M, Minabe Y, Lewis DA, Hashimoto T. Cortical Gene Expression after a Conditional Knockout of 67 kDa Glutamic Acid Decarboxylase in Parvalbumin Neurons. Schizophr Bull. 2016
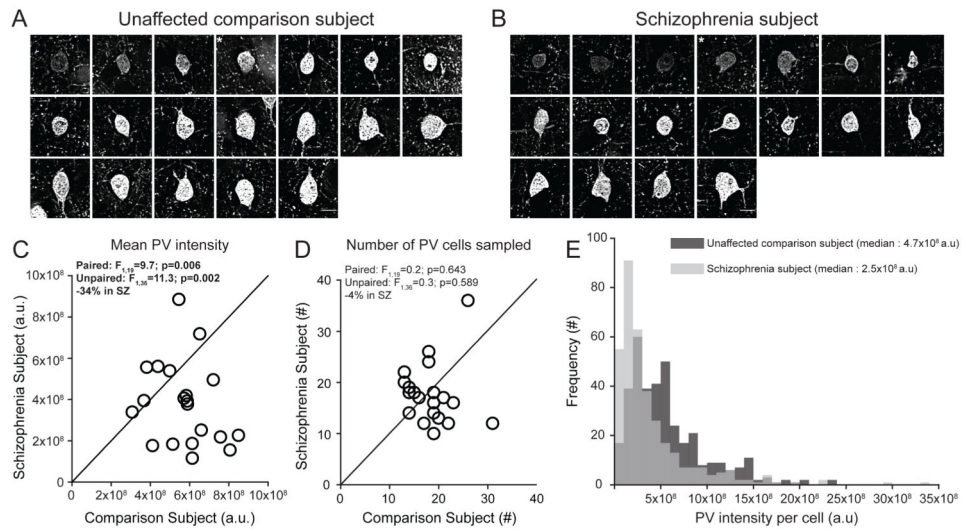
Figure 1.
Sampling of PV+ neurons and the quantification of PV immunoreactivity levels in DLPFC area 9 for each matched pair of unaffected comparison and schizophrenia subjects[a]

[a] Panels A and B illustrate the representative sampling of PV+ neurons with varying range of PV intensity levels from one subject pair (Hu1543 and Hu10026, see Supplementary Table S1). Images show a Z-plane that contains the largest surface area of PV+ cell body. * denotes PV+ neurons shown in Figure 2. Scale bars = 10 μm. In panels C and D, the scatter plots indicate the levels of dependent measures (indicated in the heading of each graph) for each unaffected comparison and schizophrenia subject in a pair (open circles). Data points below the diagonal unity line indicate a lower level in the schizophrenia subject relative to the matched unaffected comparison subject. Statistics from both paired and unpaired ANCOVA analyses are shown for each dependent measure. Mean ($\pm$SD) somal PV immunoreactivity levels in PV+ cell bodies were significantly lower in schizophrenia subjects relative to unaffected comparison subjects (panel C; schizophrenia: $3.8\times10^8\pm2.0\times10^8$, comparison: $5.7\times10^8\pm1.5\times10^8$), whereas the mean ($\pm$SD) numbers of PV+ neurons sampled did not differ between subject groups (panel D; schizophrenia: 17.7 ± 6.0, comparison: 18.5 ± 4.6). Panel E illustrates the frequency distributions of somal PV intensity values of PV+ neurons sampled from schizophrenia subjects (light gray) and unaffected comparison subjects (dark gray). Each bin represents 1×10^8 a.u..
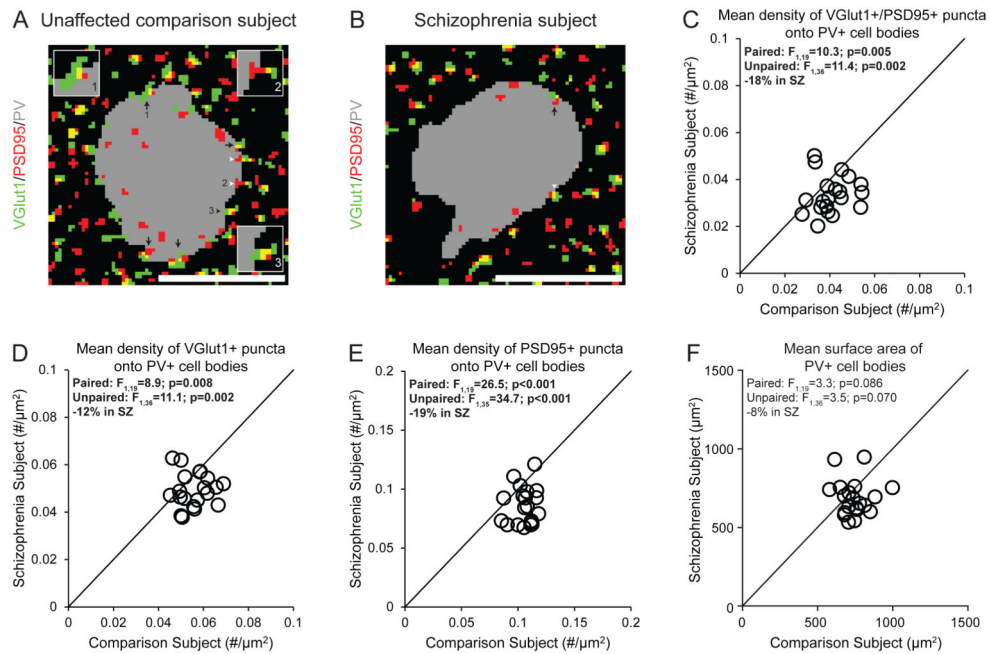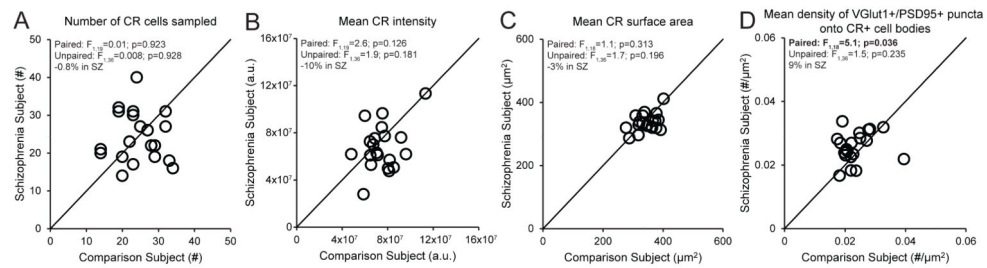
Figure 2.
Lower density of excitatory synapses on PV+ neurons in schizophrenia subjects relative to matched unaffected comparison subjects [a]

[a] Panels A and B illustrate representative masked images of VGlut1+ puncta (green), PSD95+ puncta (red) and PV+ cell bodies (gray) from the subject pair shown in Figure 1A and B. Excitatory synapses on PV+ neurons were identified by the overlap of VGlut1+/PSD95+ puncta (yellow) within a PV+ cell body (black arrows, inset image #1). Overlapping VGlut1+/PSD95+ where only the PSD95+ puncta (white arrowheads, inset image #2) or VGlut1+ puncta (black arrowheads, inset image #3) were located within a PV cell body were not included as excitatory synapses. Scale bars = 10 μm. In panels C-F, the scatter plots indicate the levels of dependent measures (indicated in the heading of each graph) for each unaffected comparison and schizophrenia subject in a pair. Mean (±SD) density of VGlut1+/PSD95+ puncta (panel C; schizophrenia: 0.0335±0.008, comparison: 0.0409±0.008), VGlut1+ puncta (panel D; schizophrenia: 0.0492±0.007, comparison: 0.0558±0.007) and PSD95+ puncta (panel E; schizophrenia: 0.0857±0.016, comparison: 0.106±0.010) on PV+ cell bodies were all significantly lower in schizophrenia subjects relative to unaffected comparison subjects. Mean (±SD) surface area of PV+ cell bodies did not differ between subject groups (panel F; schizophrenia: 684±111, comparison: 745±96).
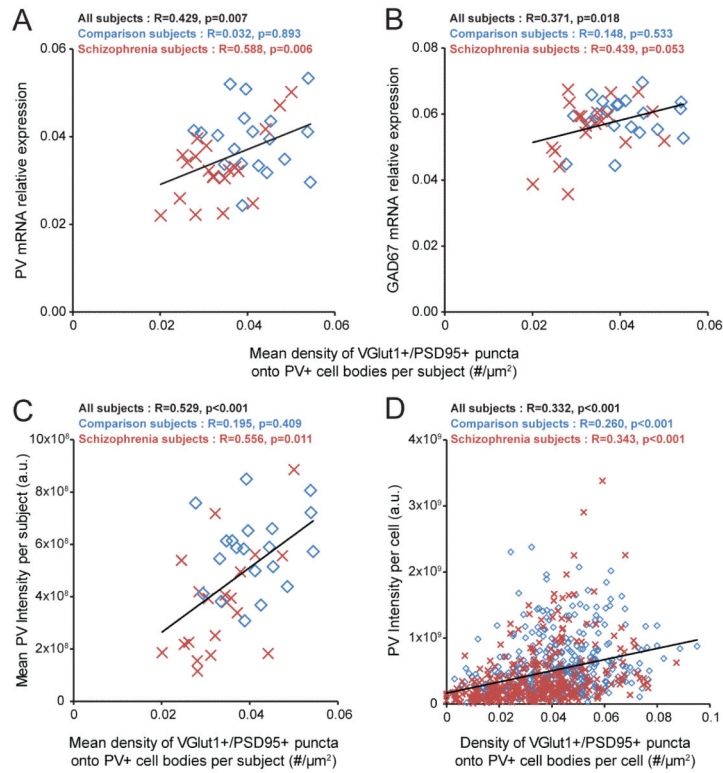
Figure 3.

Quantification of excitatory synapses on CR+ neurons in DLPFC area 9 for each matched pair of unaffected comparison and schizophrenia subjects[a]

[a] In panels A-D, the scatter plots indicate the levels of dependent measures (indicated in the heading of each graph) for each unaffected comparison and schizophrenia subject in a pair. Mean (±SD) numbers of sampled CR+ neurons (panel A; schizophrenia: 24.3±6.7, comparison: 24.5±5.9), CR immunoreactivity levels in CR+ cell bodies (panel B; schizophrenia: $6.8\times10^7\pm2.0\times10^7$, comparison: $7.5\times10^7\pm1.5\times10^7$) or surface area of CR+ cell bodies (panel C; schizophrenia: 336±28, comparison: 347±34) did not differ between subject groups. Mean (±SD) density of VGlut1+/PSD95+ puncta on CR+ cell bodies was slightly higher in schizophrenia subjects relative to unaffected comparison subjects (panel D; schizophrenia: 0.0257±0.005, comparison: 0.0236±0.005).

Figure 4.
Association between the density of excitatory synapses on PV+ neurons and activity-
dependent expression levels of PV and GAD67 selectively in schizophrenia subjects[a]
[a] In panels A and B, PV and GAD67 mRNA expression levels are plotted against the density
of VGlut1+/PSD95+ puncta on PV+ cell bodies across subjects. The mean density of
VGlut1+/PSD95+ puncta on PV+ cell bodies positively predicted the relative mRNA levels
of PV (panel A) and GAD67 (panel B) in the schizophrenia subjects and not in the
comparison subjects. In panels C and D, somal PV immunoreactivity levels are plotted
against the density of VGlut1+/PSD95+ puncta on PV+ cell bodies across subjects or across
all sampled PV+ neurons. Across subjects, the mean density of VGlut1+/PSD95+ puncta on
PV+ cell bodies positively predicted the mean somal PV immunoreactivity levels in the
schizophrenia subjects but not in the comparison subjects (panel C). Across all sampled PV+
neurons (N=725), the density of VGlut1+/PSD95+ puncta on PV+ cell bodies positively
predicted somal PV immunoreactivity levels (panel D). Diamonds (blue): unaffected
comparison subjects. Crosses (red): schizophrenia subjects. Trendlines (black): regression
lines across all subjects.

Table 1

Summary characteristics of human subjects used in this study

Characteristic	Unaffected comparison		Schizophrenia		
Sex	**N**	**%**	**N**	**%**	
Male	15	75	15	75	
Female	5	25	5	25	
Race	**No**	**%**	**No**	**%**	
White	16	80	14	70	
Black	4	20	6	30	
	Mean	**SD**	**Mean**	**SD**	**Paired T-test statistics**
Age (years)	46.3	12.1	45.2	11.8	t_{19}=1.3, p=0.209
Postmortem interval (hours)	16.4	5.5	15.4	6.3	t_{19}=0.7, p=0.470
Freezer storage time (months)	110.8	33.9	103.5	28.3	t_{19}=0.9, p=0.355